



OPEN

Unexpected Magnetic Semiconductor Behavior in Zigzag Phosphorene Nanoribbons Driven by Half-Filled One Dimensional Band

SUBJECT AREAS:
MAGNETIC PROPERTIES
AND MATERIALS
ELECTRONIC STRUCTUREReceived
22 October 2014Accepted
29 January 2015Published
9 March 2015Yongping Du^{1*}, Huimei Liu^{1*}, Bo Xu², Li Sheng^{1,4}, Jiang Yin², Chun-Gang Duan³ & Xiangang Wan^{1,4}

¹National Laboratory of Solid State Microstructures, and Department of Physics, Nanjing University, Nanjing, 210093, China, ²National Laboratory of Solid State Microstructures and Department of Materials Science and Engineering, Nanjing University, Nanjing, 210093, China, ³Key Laboratory of Polar Materials and Devices, Ministry of Education, East China Normal University, Shanghai 200062, China, ⁴Collaborative Innovation Center of Advanced Microstructures, Nanjing University, Nanjing 210093, China.

Correspondence and requests for materials should be addressed to X.W. (xgwan@nju.edu.cn) or B.X. (xubonju@gmail.com)

* These authors contributed equally to this work.

Phosphorene, as a novel two-dimensional material, has attracted a great interest due to its novel electronic structure. The pursuit of controlled magnetism in Phosphorene in particular has been persisting goal in this area. In this paper, an antiferromagnetic insulating state has been found in the zigzag phosphorene nanoribbons (ZPNRs) from the comprehensive density functional theory calculations. Comparing with other one-dimensional systems, the magnetism in ZPNRs display several surprising characteristics: (i) the magnetic moments are antiparallel arranged at each zigzag edge; (ii) the magnetism is quite stable in energy (about 29 meV/magnetic-ion) and the band gap is big (about 0.7 eV); (iii) the electronic and magnetic properties is almost independent on the width of nanoribbons; (iv) a moderate compressive strain will induce a magnetic to nonmagnetic as well as semiconductor to metal transition. All of these phenomena arise naturally due to one unique mechanism, namely the electronic instability induced by the half-filled one-dimensional bands which cross the Fermi level at around $\pi/2a$. The unusual electronic and magnetic properties in ZPNRs endow them possible potential for the applications in nanoelectronic devices.

Since the experimental realization of graphene nanoribbons by cutting graphene into nanometer-sized width¹, the electronic and magnetic properties of nanoribbon have raised a lot of attention^{1–12}. Especially, the zigzag graphene nanoribbons (ZGNRs) were predicted to be antiferromagnetic semiconductors by noticing the two fold degenerated flat energy band at the Fermi level^{2,3}. Moreover, it had been proposed that the half-metallicity in ZGNRs can be realized under an external transverse electric field^{4,5}, while many other methods, such as doping⁶, defects⁷ and edge-modification^{8,9} were applied to tune or control the magnetism in ZGNRs. Partial theoretical predictions had been confirmed by the experiment^{10,11}. In addition to graphene nanoribbons, magnetism had also been proposed for several other nanoribbons, such as BN¹³, MoS₂¹⁴ and ZnO¹⁵. However, for ZGNRs the electronic and magnetic properties strongly depend on the ribbon width², while the metallicity in magnetic MoS₂¹⁴ and ZnO¹⁵ nanoribbons limits their applications in nanoscale electronic devices.

Recently, a new two dimensional (2D) material, layered black phosphorus (phosphorene)^{16–21}, has been isolated in the laboratory through mechanical exfoliation from bulk black phosphorus. It was reported that phosphorene has carrier mobility up to 1000 cm²/V·s¹⁶ and an appreciably high on/off ratio of 10000 in phosphorene transistor at room temperature¹⁷, which makes phosphorene a potential candidate for future nanoelectronic applications^{16–32}. Numerical calculation found that phosphorene is an insulator with direct bandgap, a 3% in-plane strain can change phosphorene to an indirect-gap semiconductor¹⁷, while a vertical compression can induce a semiconductor to metal transition²². The properties of phosphorene nanoribbons (PNRs), especially zigzag phosphorene nanoribbons (ZPNRs) and armchair phosphorene nanoribbons (APNRs) have also been studied^{25–29}. It had been found that similar with phosphorene, the tensile stain and electric-field can modulate the physical properties of PNRs^{25,28}. The possible structural reconstruction in the edge of PNRs had also been investigated²⁹. As an alternative material to graphene, a lot of properties of phosphorene and PNRs, such as



thermal, mechanic and electronic, have been extensively investigated^{24,33,34}. But no evidence of formation of magnetic order at the phosphorene or PNRs has been reported so far. Thus the study of the intrinsic magnetism in phosphorene or PNRs to date is inconclusive and it is desirable to seek the magnetism in phosphorene nanostructures.

Carefully inspecting the electronic band structure, we find that except those with very narrow width, ZPNRs always have two well-defined edge states. These edge states are exactly half-filled and cross the Fermi level almost at $k = \pi/2a$ (a is the lattice parameter along the periodic direction of ribbon), consequently induce a giant instability as will be discussed later. We demonstrate that driven by this instability, the ground state of ZPNRs is antiferromagnetic (AFM) semiconductor. Compared with other magnetic nanoribbons, ZPNRs are semiconductors, their band gap, magnetic moment and the energy difference between the magnetic state and the non-magnetic (NM) state are almost independent on the ribbon width. We also find that a moderate compressive strain will make the edge state crossing the Fermi level twice, which reduces the amplitude of susceptibility anomaly, thus results in a magnetic to nonmagnetic and semiconductor to metal transition. The stable and tunable electronic and magnetic properties in ZPNRs endow them great potential for the applications in nanoscale electronic devices.

Results

Geometries of zigzag phosphorene nanoribbons. The relaxed lattice constants in our HSE06 calculation for monolayer phosphorene are $a = 3.29 \text{ \AA}$, $b = 4.51 \text{ \AA}$, in good agreement with other theoretical calculations^{17,25}. Following the convention about the GNRs^{2,3}, the ZPNRs are classified by the number of sawlike lines across the ribbon width as shown in Figure 1(a). It had been found that the edge states of the narrow ZPNRs are strongly hybridized together, we thus focus on the ribbons with width larger than 8, where the edge states are well defined, and the

electronic structure and magnetic properties are almost not dependent on the width of ribbon. Upon structure relaxations, we find that the bond $b1$, which connects the edge P atom and P atoms in the interior of the nanoribbon as shown in Figure 1(a), decreases from 2.22 \AA to 2.14 \AA for 8-ZPNR. The corresponding edge angles α and β increase from 96.3° to 100.9° , and from 102.1° to 108.8° , respectively. Similar structural change has also been found for other ZPNRs with different width, in consistent with the previous calculations²⁵.

Ground state of zigzag phosphorene nanoribbons and its mechanism.

We perform non-spin-polarized calculation to check the basic electronic feature of ZPNRs. Consistent with other theoretical results²⁵, our HSE06 calculation also find that there are two bands crossing the Fermi level shown as the red lines in Figure 1(b). Those bands are quite separated from bulk ones and basically are pure edge states. It is interesting to see that those edge bands are quite narrow. For 8-ZPNR, the bandwidth is about 1.60 eV as shown in Figure 1(b), and the bandwidth will decrease slightly with increasing ribbon width as shown in Figure 1(c). Consistent with previous theoretical work²⁵, our HSE06 calculations also find that the two edge bands are nearly degenerate around the zone boundary, and have considerable split at Γ point. Increasing the width of ZPNRs will reduce the interaction between two edges thus lead to the decrease of the edge state split at Γ point as shown in Figure 1(c). The most peculiar character of the electronic structure of ZPNRs with the width larger than 8 is that the well defined edge states are one-dimensional, exactly half-filled due to only one dangling bond per edge atom in the ZPNRs. The edge states are nearly degenerate in more than half of the Brillouin zone, consequently the half-filled band cross the Fermi level almost exactly at $\pi/2a$ as shown in Figure 1(b).

Here we demonstrate that such behavior of the edge state may bring exotic physical property to ZPNRs. Let us first study the famous Lindhard function $(\text{LF})_{xq} = \sum_k \frac{f(k) - f(k+q)}{\varepsilon_{k+q} - \varepsilon_k}$, which

describes the bare electronic susceptibility and plays a crucial role in determining the structural and electronic properties of the system. In this expression, $f(k)$ denotes the Fermi-Dirac distribution function, while ε_k is the electron energy of the momentum $\hbar k$. It is well known that for 1D state, due to the effect of denominator, the susceptibility exhibits a large anomaly for $q = 2K_F$, where K_F is the wave vector on the Fermi surface³⁵. In addition to the effect of denominator, we find that for ZPNRs, the numerator in LF also play important role³⁶. Due to the requirement from $f(k)$, the nonzero contribution to the numerator can only come from those k and $k + q$ in and out of the Fermi sea, respectively, and the integration of the numerator alone actually only depends on K_F and q . For a given K_F , the maximum value of the integration of the numerator in the LF (i.e., the available phase-space area) can be expressed as:

$$\max\left(\sum_k (f(k) - f(k+q))\right) = \begin{cases} 2K_F \dots (K_F < \frac{\pi}{2a}) \\ \frac{\pi}{a} \dots (K_F = \frac{\pi}{2a}) \\ \frac{2\pi}{a} - 2K_F \dots (K_F > \frac{\pi}{2a}) \end{cases} \quad (1)$$

Here we note that a too large value $k + q$ will again falls into the Fermi sphere due to the periodicity. When $K_F \sim \pi/2a$, as ZPNRs do, the integration of the numerator also reaches a maximum value at the same $q = 2K_F \sim \pi/a$ point, where χ_q exhibits a singular behavior due to the effect of denominator. These two jointed effects result in abnormal behavior of χ_q at $q = \pi/2a$, which strongly suggests that there exists giant instability in ZPNRs at NM state.

To check the possible magnetic instability, we double the unit cell along the periodic direction, and perform the spin-polarized calculation.

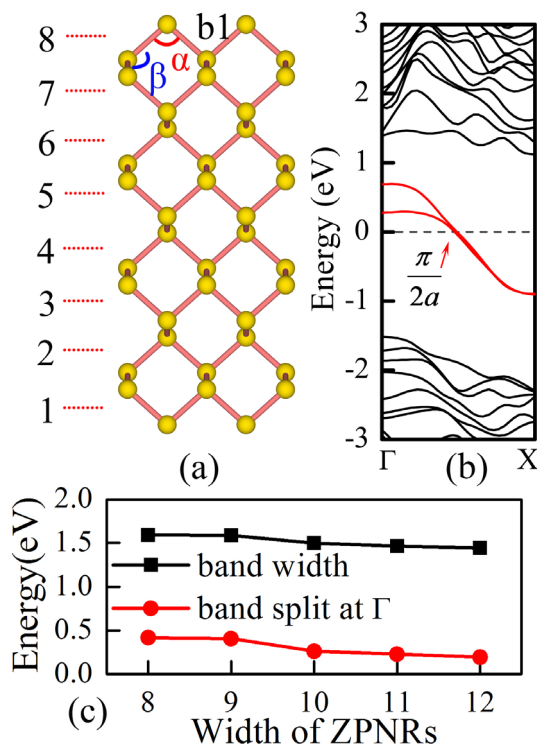


Figure 1 | (a) Ball-and-stick model of 8-ZPNR; (b) Band structure of 8-ZPNR calculated by HSE06 scheme; (c) Back line denotes the band width as the function of ribbon width, red line is the band split at the Γ point as the function of ribbon width.

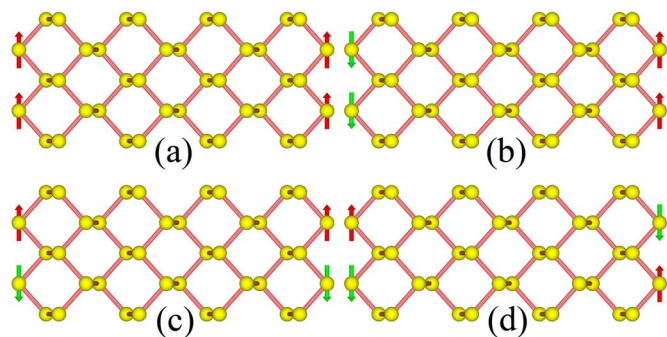


Figure 2 | The initial magnetic structures adopt for searching ground state (a) FM order; (b) AFM-1 order; (c) AFM-2 order; (d) AFM-3 order.

tion for the ZPNRs with widths from 8 to 12. We select four magnetic configurations: ferromagnetic (FM), intra-edge FM and inter-edge AFM (AFM-1), intra-edge AFM and inter-edge FM (AFM-2), intra-edge AFM and inter-edge AFM order (AFM-3), as shown in Figure 2. We first perform calculation for 8-ZPNR, and find that FM and AFM-1 configurations are unstable and always converge to NM states finally. On the other hand, the intra-edge AFM configurations are energetically more favorable than the NM. We find that the AFM-2 configuration is the ground state, and is about 108.89 meV lower in energy than the NM state as listed in Table 1. As shown in Figure 3(a), the magnetic moments are mainly located at the edge sites. The AFM-3 configuration is just 0.37 meV higher than the AFM-2 state, which indicates that the magnetic interaction between the two edges is very small and the large energy gain (about 109 meV) basically comes from the formation of AFM ordering along the edge.

Influence of ribbon width on AFM coupling. We also calculate a series of N-ZPNRs (N from 9 to 12), and find that regardless the ribbon width, the FM and AFM-1 configurations are not stable. The energy difference between the AFM-2 and AFM-3 approach to zero with increasing the ribbon width, which again indicates that the inter-edge magnetic interaction is very weak. The AFM-2 and AFM-3 are almost degenerate in energy, and their electronic bands are also almost the same, thus the energy difference between the magnetic state and NM is an important value, which is close to 115 meV as shown in Figure 4(c). As shown in Figure 3(a), there are basically four magnetic sites, thus the energy gain per site is about 29 meV, which is higher than many other 1D cases^{13,14}. As displayed in Figure 4, the magnetic moment at the edge atoms (around 0.155 μ_B) also hardly depend on the ribbon width.

Influence of strain on electronic and magnetic properties. It is interesting to see that accompanying with the formation of AFM order at the edge, the edge bands split and the compound becomes a direct gap semiconductor with a sizable band gap (about 0.7 eV) opened for 8-ZPNR as shown in Figure 3(b). Moreover, we have also computed the band structures of a series of N-ZPNRs (N from 9 to 12), they are all semiconductor, and their band gaps are weakly dependent on the nanoribbon width as presented in Figure 4(a). It is very interesting that the hole effective mass of nanoribbons MoS₂ show a strong oscillation behavior³⁷. Promoting by these unique results, we calculated the effective mass of ZPNRs. The calculated hole effective masses are $-0.514 m_e$ and $-0.542 m_e$ for 8-ZPNRs

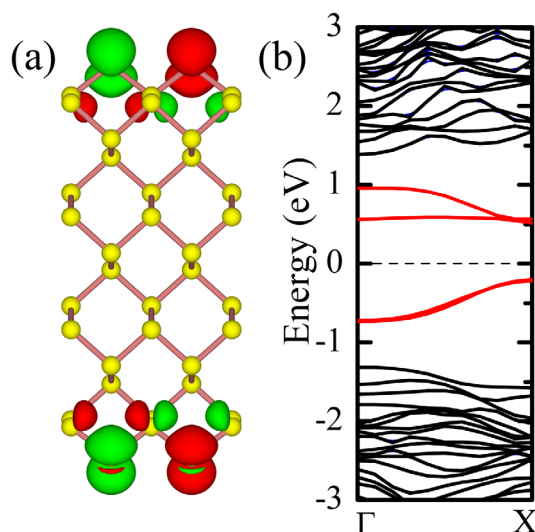


Figure 3 | (a) Spatial spin distribution of 8-ZPNR, the red one denote the spin up and green one is the spin down with the isosurface value 0.002 $e/\text{\AA}^3$; (b) Band structure of 8-ZPNR with AFM-2 configuration.

and 10-ZPNRs, respectively. These results indicate that the hole effective mass of ZPNRs is not sensitive to the ribbon width. The evolution of the electron effective mass with the ribbon width was similar to the one of hole. As pointed out above, the insulating AFM state of ZPNR arises from the strong instability induced by the 1D half-filled bands which cross the Fermi level at around $\pi/2a$, thus it is natural to expect that the electronic and magnetic properties will change dramatically if one can tune the edge states. As well known, the edge states usually are sensitive to strain, doping, and external field. Here we focus on the effect of strain on the edge states.

To analyze the effect of the compressive strains along the periodic direction, we display the electron structure of the edge state. As shown in Figure 5(b), (c), and (d), consistent with the previous theoretical results²⁵, we find that the compressive strains has small effect on the bandwidth. Consequently, both the magnetic moment and the energy difference between the magnetic ground state and the NM state are not sensitive to small strains as shown in the Figure 5(a). The main influence of the compressive strains on the band structure is to enlarge the edge states splitting at Γ point, and after a critical compressive strain (about 5%), the edge states will cross the Fermi level twice as shown in Figure 5(c). This will reduce the amplitude of the susceptibility anomaly at $q = \pi/a$. Consistent with that, our calculations show that now the ground state change from AFM semiconductor to nonmagnetic metal. We also perform calculation for other ribbon width, and find that regardless the width, a moderate strain (around 5%) always induce a magnetic to nonmagnetic and semiconductor to metal transition. We also checked the effect of tensile strain. Similar to compressive strain, a tensile strain of 5% can also tune the AFM semiconductor to nonmagnetic metal. The monolayer phosphorene can sustain a large tensile strain up to 27% as reported by Wei et al.³⁸. It is much larger than the critical strain for the semiconductor-metal transition (5%), thus it is reasonable to expect that the transition would survive under the strain. In addition to the instability around $q = \pi/a$, basically we also need to check the instability induced by the Fermi surface around Γ point.

Table 1 | Total energy and magnetic moment of different magnetic configurations of 8-ZPNR

8-ZPNR	NM	FM	AFM-1	AFM-2	AFM-3
Energy(meV)	108.89	108.89	108.89	0.0	0.37
Magnetic moment(μ_B)	0	0	0	0.151	0.152

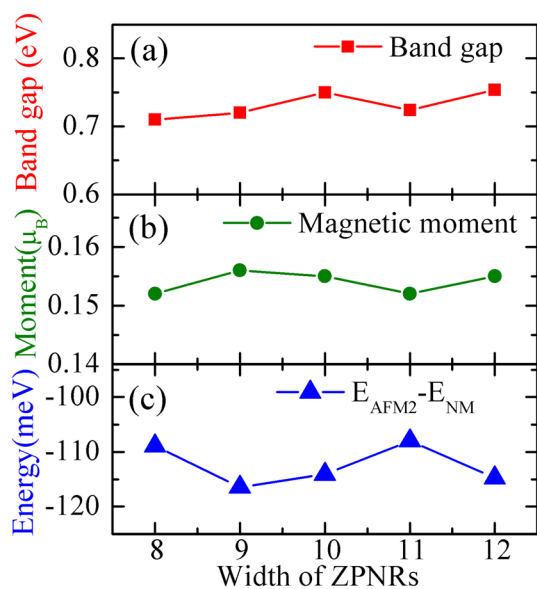


Figure 4 | Electronic and magnetic properties of a series of N-ZPNRs (N = 8 to 12): (a) band gap and (b) magnetic moment of ZPNR with AFM-2 configuration as the function of ribbon width; (c) energy differences between the NM state and AFM-2 ground state change with the ribbon width.

Unfortunately, as shown in Figure 5(b), this point is far from any simple fraction. Such incommensurate-like phase currently is beyond our ability to handle. We, however, believe this kind of ordering is unlikely to occur, due to the fact that the amplitude of χ_q at this point is smaller than that at $q = \pi/a$.

Discussion

Due to the above discussed unique mechanism, the magnetic properties in ZPNRs are quite different with other magnetic nanoribbon systems. The magnetism of ZPNRs arises from the sites located at two edges, and along the edge the magnetic moment are AFM ordered, therefore we do not expect that transverse electric field will

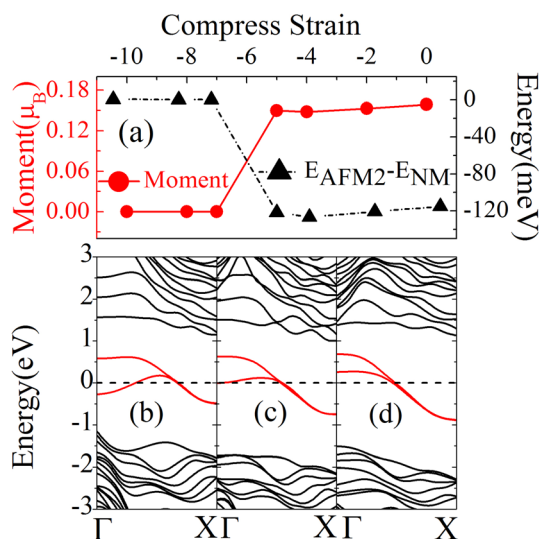


Figure 5 | Effect of compressive strain on the magnetic and electronic properties of ZPNRs. (a) The dash line with black triangle is the energy difference between NM state and AFM-2 state, and the magnetic moment is shown by red line with solid circle; (b) (c) (d) are the band structures of 8-ZPNR under the compressive strain of 10%, 5%, 0%, respectively.

induce AFM semiconductor to NM metal transition, which is different from the case in ZGNRs⁵. Whereas the edge is FM ordered for ZGNRs², the magnetic moment in zigzag ZnO nanoribbon is only contributed by the oxygen edge¹⁵, and for zigzag MoS₂ ribbon the magnetic moments of both inter- and intra-edge are FM coupled¹⁴. In addition, ZPNRs have following advantages: (i) the energy difference between magnetic ground state and NM state is around 29 meV/magnetic-site, which is substantially larger than that of ZGNRs and MoS₂ nanoribbon. The rather stable magnetism in ZPNRs is very important for the electronic devices application at room temperature; (ii) the magnetic and electronic properties of ZPNRs are almost independent on the width of nanoribbons, which is a great advantage for their applications; (iii) a moderate in-plane compression, possibly caused by epitaxial mismatch with a substrate, can induce a sharp magnetic to nonmagnetic as well as a semiconductor to metal transition.

In addition to the magnetism, the anomaly of susceptibility may also result in a charge-density-wave (CDW) like distortion. We thus again double the cell along the periodic direction and relax both the lattice constant and internal coordinates of ZPNRs to check the possible structural reconstruction. We find that the ZPNRs maintain the original unit cell in the axis of ribbon and do not exhibit the Peierls like distortion. The possible edge reconstruction had also been discussed by Maity *et al.*²⁹, the energy gain of the structural distortion is only 0.6 meV/atom, which is close to the limits of density functional calculation²⁹, and also much less than the energy gain of magnetism as discussed at above. We thus believe the CDW transition will not occur, and there is no edge reconstruction for ZPNRs. In addition to the magnetic and structural transition discussed above, superconductivity is another possibility to remove the instability, we therefore invoke experimental efforts to study this possible rare 1D superconductor.

In summary, we have presented a detailed study on the intrinsic magnetic properties of ZPNRs. In graphene, the edge magnetism originated from the Lieb theorem of bipartite lattice, so that A sub-lattices and B sub-lattices are FM coupled within themselves, but A and B are always AFM coupled with each other. As a result, one can design the edge magnetism by following a simple design principle based on the zigzag edge orientation¹². In PNRs, We demonstrate that this magnetic properties originate from the instability induced by the half-filled one-dimensional bands crossing the Fermi level. So, the magnetism could be realized in other PNRs, such as diagonal phosphorene nanoribbons, by introducing the half-filled one dimensional band. Our findings not only reveal for the first time possibility of magnetism in PNRs, but also open up an opportunity to realize spintronics at the atomical thin single-layer level, in which controlled magnetism may be achieved by strain.

Method

Our density functional calculations were based on the Vienna ab initio simulation package (VASP)^{39,40}. An energy cutoff of 500 eV was adopted for the plane-wave expansion of the electronic wave function and the energy convergence criteria was set to 10^{-5} eV. To sample the Brillouin zone, appropriate k-point meshes of (9*1*1) were used for calculations. Structures were relaxed until the force on each atom was less than 0.01 eV/Å. It is well known that the local (local density approximation) or semi-local (generalized gradient approximation) approximations for the electronic exchange and correlation fail to cancel the self-interaction error⁴¹. On the other hand, with the correction of the SIE, hybrid function scheme had been shown are superior to the LDA and GGA in description of not only the lattice structure but also the electronic and magnetic properties⁴²⁻⁴⁶. Thus in this work, we apply the hybrid function of HSE06^{45,46} to investigate the electronic band structure and magnetic properties of phosphorene nanoribbons. A vacuum spacing of 18 Å is used so that the interaction in the non-periodic directions can be neglected.

1. Wang, X. R. *et al.* N-Doping of Graphene Through Electrothermal Reactions with Ammonia. *Science* **324**, 768 (2009).
2. Son, Y. W., Cohen, M. L. & Louie, S. G. Energy Gaps in Graphene Nanoribbons. *Phys. Rev. Lett.* **97**, 216803 (2006).



3. Fujita, M., Wakabayashi, K., Nakada, K. & Kusakabe, K. Peculiar Localized State at Zigzag Graphite Edge. *J. Phys. Soc. Jpn.* **65**, 1920 (1996).
4. Son, Y. W., Cohen, M. L. & Louie, S. G. Half-metallic graphene nanoribbons. *Nature* **444**, 347 (2006).
5. Wang, Z. F., Jin, S. & Liu, F. Spatially Separated Spin Carriers in Spin-Semiconducting Graphene Nanoribbons. *Phys. Rev. Lett.* **111**, 096803 (2013).
6. Li, Y. F., Zhou, Z., Shen, P. & Chen, Z. F. Spin Gapless Semiconductor-Metal-Half-Metal Properties in Nitrogen-Doped Zigzag Graphene Nanoribbons. *ACS Nano* **3**, 1952 (2009).
7. Lin, X. & Ni, J. Half-metallicity in graphene nanoribbons with topological line defects. *Phys. Rev. B* **84**, 075461 (2011).
8. Kan, E. J., Li, Z., Yang, J. & Hou, J. G. Half-Metallicity in Edge-Modified Zigzag Graphene Nanoribbons. *J. Am. Chem. Soc.* **130**, 4224 (2008).
9. Xu, B. *et al.* Electronic and magnetic properties of zigzag graphene nanoribbon with one edge saturated. *Appl. Phys. Lett.* **96**, 163102 (2010).
10. Li, X. L., Wang, X. R., Zhang, L., Lee, S. W. & Dai, H. J. Chemically Derived, Ultrasmooth Graphene Nanoribbon Semiconductors. *Science* **319**, 1229 (2008).
11. Ritter, K. A. & Lyding, J. W. The influence of edge structure on the electronic properties of graphene quantum dots and nanoribbons. *Nat. Mater.* **8**, 235 (2009).
12. Yu, D. C., Lupton, E. M., Gao, H. J., Zhang, C. & Liu, F. A unified geometric rule for designing nanomagnetism in graphene. *Nano Res.* **1**, 497 (2008).
13. Barone, V. & Peralta, J. E. Magnetic Boron Nitride Nanoribbons with Tunable Electronic Properties. *Nano Lett.* **8**, 2210 (2008).
14. Li, Y. F., Zhou, Z., Zhang, S. B. & Chen, Z. F. MoS₂ Nanoribbons: High Stability and Unusual Electronic and Magnetic Properties. *J. Am. Chem. Soc.* **130**, 16739 (2008).
15. Botello-Méndez, A. R., López-Urías, F., Terrones, M. & Terrones, H. Magnetic Behavior in Zinc Oxide Zigzag Nanoribbons. *Nano Lett.* **8**, 1562 (2008).
16. Li, L. *et al.* Black phosphorus field-effect transistors. *Nat. Nanotech.* **9**, 372 (2014).
17. Liu, H., Neal, A. T., Zhu, Z., Tománek, D. & Ye, P. D. Phosphorene: An Unexplored 2D Semiconductor with a High Hole Mobility. *ACS Nano* **8**, 4033 (2014).
18. Eugenie, S. R. Phosphorene excites materials scientists. *Nature* **506**, 19 (2014).
19. Li, W. F., Zhang, G. & Zhang, Y. W. Electronic Properties of Edge-Hydrogenated Phosphorene Nanoribbons: A First-Principles Study. *J. Phys. Chem. C* **118**, 22368 (2014).
20. Ong, Z. Y., Cai, Y. Q., Zhang, G. & Zhang, Y. W. Strong Thermal Transport Anisotropy and Strain Modulation in Single-Layer Phosphorene. *J. Phys. Chem. C* **118**, 25272(2014).
21. Cai, Y. Q., Zhang, G. & Zhang, Y. W. Layer-dependent Band Alignment and Work Function of Few-Layer Phosphorene. *Sci. Rep.* **4**, 6677(2014).
22. Rodin, A., Carvalho, A. & Neto, A. H. C. Strain-Induced Gap Modification in Black Phosphorus. *Phys. Rev. Lett.* **112**, 176801 (2014).
23. Qiao, J. S., Kong, X. H., Hu, Z. X., Yang, F. & Ji, W. High-mobility transport anisotropy and linear dichroism in few-layer black phosphorus. *Nat Commun.* **5**, 4475 (2014).
24. Dai, J. & Zeng, X. C. Bilayer Phosphorene: Effect of Stacking Order on Bandgap and Its Potential Applications in Thin-Film Solar Cells. *J. Phys. Chem. Lett.* **5**, 1289 (2014).
25. Guo, H., Lu, N., Wang, L., Wu, X. & Zeng, X. C. Phosphorene Nanoribbons, Phosphorus Nanotubes, and van der Waals Multilayers. *J. Phys. Chem. C* **118**, 14051 (2014).
26. Tran, V. & Yang, L. Scaling laws for the band gap and optical response of phosphorene nanoribbons. *Phys. Rev. B* **89**, 245407 (2014).
27. Carvalho, A., Rodin, A. S. & Neto, A. H. C. Phosphorene nanoribbons. *arXiv:1404.5115* (2014).
28. Han, X. Y., Stewart, H. M., Shevlin, S. A., Catlow, C. R. A. & Guo, Z. X. Strain and Orientation Modulated Bandgaps and Effective Masses of Phosphorene Nanoribbons. *Nano Lett.* **14**, 4607 (2014).
29. Maity, A., Singh, A. & Sen, P. Peierls transition and edge reconstruction in phosphorene nanoribbons. *arXiv:1404.2469v2* (2014).
30. Zhu, Z. & Tománek, D. Semiconducting Layered Blue Phosphorus: A Computational Study. *Phys. Rev. Lett.* **112**, 176802 (2014).
31. Wu, Q. Y., Shen, L., Yang, M., Huang, Z. G. & Feng, Y. P. Band Gaps and Giant Stark Effect in Nonchiral Phosphorene Nanoribbons. *arXiv:1405.3077* (2014).
32. Fei, R. & Yang, L. Strain-Engineering the Anisotropic Electrical Conductance of Few-Layer Black Phosphorus. *Nano Lett.* **14**, 2884 (2014).
33. Das, S. *et al.* Tunable Transport Gap in Phosphorene. *Nano Lett.* **14**, 5733 (2014).
34. Xia, F., Wang, H. & Jia, Y. Rediscovering black phosphorus as an anisotropic layered material for optoelectronics and electronics. *Nature Comm.* **5**, 4458 (2014).
35. Peierls, R. E. *Quantum theory of solids* (Clarendon, Oxford 1955).
36. Oudovenko, V. S., Savrasov, S. Y. & Andersen, O. K. On the Fermi surface geometry and antiferromagnetism of YBa₂Cu₃O_{6+x}. *Physica C* **336**, 157 (2000).
37. Cai, Y. Q., Zhang, G. & Zhang, Y. W. Polarity-Reversed Robust Carrier Mobility in Monolayer MoS₂ Nanoribbons. *J. Am. Chem. Soc.* **136**, 6269 (2014).
38. Wei, Q. & Peng, X. Superior mechanical flexibility of phosphorene and few-layer black Phosphorus. *Appl. Phys. Lett.* **104**, 251915 (2014).
39. Kresse, G. & Furthmüller, J. Efficient iterative schemes for *ab initio* total-energy calculations using a plane-wave basis set. *Phys. Rev. B* **54**, 11169 (1996).
40. Kresse, G. & Furthmüller, J. Efficiency of *ab-initio* total energy calculations for metals and semiconductors using a plane-wave basis set. *Comp. Mater. Sci.* **6**, 15 (1996).
41. Kummel, S. & Kronik, L. Orbital-dependent density functionals: Theory and applications. *Rev. Mod. Phys.* **80**, 3 (2008).
42. Kim, H. J. & Cho, J. H. Fluorine-induced local magnetic moment in graphene: A hybrid DFT study. *Phys. Rev. B* **87**, 174435 (2013).
43. Chevrier, V. L., Ong, S. P., Armiento, R., Chan, M. K. Y. & Ceder, G. Hybrid density functional calculations of redox potentials and formation energies of transition metal compounds. *Phys. Rev. B* **82**, 075122 (2010).
44. Schlipf, M., Betzinger, M., Ležaić, M., Friedrich, C. & Blügel, S. Structural, electronic, and magnetic properties of the europium chalcogenides: A hybrid-functional DFT study. *Phys. Rev. B* **88**, 094433 (2013).
45. Heyd, J., Scuseria, G. E. & Ernzerhof, M. Hybrid functionals based on a screened Coulomb potential. *J. Chem. Phys.* **118**, 8207 (2003).
46. Heyd, J. & Scuseria, G. E. Assessment and validation of a screened Coulomb hybrid density functional. *J. Chem. Phys.* **120**, 7274 (2004).

Acknowledgments

We acknowledge the useful discussions with S.Y. Savrasov. We acknowledge support by National Key Project for Basic Research of China (Grant No. 2011CB922101, 2013CB922301, 2014CB921104), NSFC(Grant No. 11374137, 91122035, 11204123, 11174124 and 61125403) and PAPD.

Author contributions

X.W. notices the half-filled one dimensional band in Zigzag Phosphorene Nanoribbons, and came up with the idea of checking the mechanism in this system. Y.D. and H.L. perform the calculation. X.B. and X.W. interpret the numerical results and write the paper. All authors contribute to editing the manuscript.

Additional information

Competing financial interests: The authors declare no competing financial interests.

How to cite this article: Du, Y. *et al.* Unexpected Magnetic Semiconductor Behavior in Zigzag Phosphorene Nanoribbons Driven by Half-Filled One Dimensional Band. *Sci. Rep.* **5**, 8921; DOI:10.1038/srep08921 (2015).



This work is licensed under a Creative Commons Attribution 4.0 International License. The images or other third party material in this article are included in the article's Creative Commons license, unless indicated otherwise in the credit line; if the material is not included under the Creative Commons license, users will need to obtain permission from the license holder in order to reproduce the material. To view a copy of this license, visit <http://creativecommons.org/licenses/by/4.0/>